

## DEVELOPMENT AND MONITORING OF MESOPOROUS VANADIUM CATALYSTS UNDER VISIBLE LIGHT

Yasuo Izumi, Kazushi Konishi, Dilshad Masih (Tokyo Institute of Technology, Yokohama, Japan)  
Hideaki Yoshitake (Yokohama National University, Yokohama, Japan)

**ABSTRACT:** Ethanol photo-oxidation was investigated over mesoporous (template method), sol-gel, and conventional (mainly anatase) V+TiO<sub>2</sub> catalysts. Under the illumination of visible light, mesoporous V-TiO<sub>2</sub> catalyst proceeded ethanol dehydration specific among all V+TiO<sub>2</sub> catalysts tested. Initial quicker water evolution suggested greater oxidation capability compared to other V+TiO<sub>2</sub> catalysts. To monitor the V sites in mesoporous TiO<sub>2</sub> under on-reaction condition, state-sensitive V Kβ<sub>5,2</sub>-selecting V K-edge X-ray absorption fine structure (XAFS) was applied. The red-ox states responsible for ethanol dehydration were found to V<sup>III</sup> and V<sup>IV</sup> over/in mesoporous TiO<sub>2</sub> excited in visible light. The V Kβ<sub>5,2</sub> chemical shift between V<sup>III</sup> and V<sup>IV</sup> states was 3.2 eV. Based on V Kβ<sub>5,2</sub> emission and V Kβ<sub>5,2</sub>-selecting XAFS spectra, the vanadium state was IV for fresh mesoporous V-TiO<sub>2</sub> catalyst. Due to the dissociative adsorption of ethanol under visible light, the vanadium sites were partially reduced but still in the energy range for V<sup>IV</sup> state. Partially reduced vanadium sites re-oxidized in oxygen in visible light. Finally, 60% of V<sup>III</sup> state was extracted in the V Kβ<sub>5,2</sub>-selecting XAFS tuning the fluorescence spectrometer to 5456.3 eV among the mixture of V<sup>III</sup> (minor) and V<sup>IV</sup> states (dominant) for the partially reduced mesoporous V-TiO<sub>2</sub>.

### INTRODUCTION

Utilization of solar energy is expected to be clean energy source. One of the technological possibilities is photo-catalysis over TiO<sub>2</sub>-based catalysts. Because most of light wavelength absorbable by TiO<sub>2</sub> lies in UV region, studies have been reported to shift the wavelength toward visible light region by doping with V, Cr, Mn, Fe, Ni (Anpo, 2004), C, N, or S atom (Khan et al., 2002; Aita et al., 2004) to TiO<sub>2</sub> to effectively utilize solar energy. Promoted catalysis by V doping on/in TiO<sub>2</sub> were reported for ethanol photo-oxidation (Klosek et al., 2001), degradation of crystal violet, methylene blue (Iketani et al., 2004; Wu et al., 2004), methyl orange (Hou et al., 2006), and nitric oxide (Yamashita et al., 1999) under the illumination of visible light.

In this paper, various V+TiO<sub>2</sub> catalysts were prepared via sol-gel/template synthesis and direct/two-step impregnation of V over anatase/rutile, and amorphous TiO<sub>2</sub>. Ethanol oxidation reactions were studied over the series of V+TiO<sub>2</sub> catalysts under the illumination of visible light. Further, molecular-level monitoring of the V sites and substrates under *on-reaction* conditions was performed to elucidate the specific dehydration catalysis using selective X-ray spectroscopy.

### MATERIALS AND METHODS

Mesoporous V-TiO<sub>2</sub> catalysts were prepared from V triisopropoxide oxide (1), Ti tetraisopropoxide (2), and dodecylamine (3) (Yoshitake et al., 2003). The mixture of aqueous solution was maintained at 333 K for 6 days and filtered. Obtained powder was heated at 453 K for 10 days, and washed with *p*-toluenesulfonic acid in

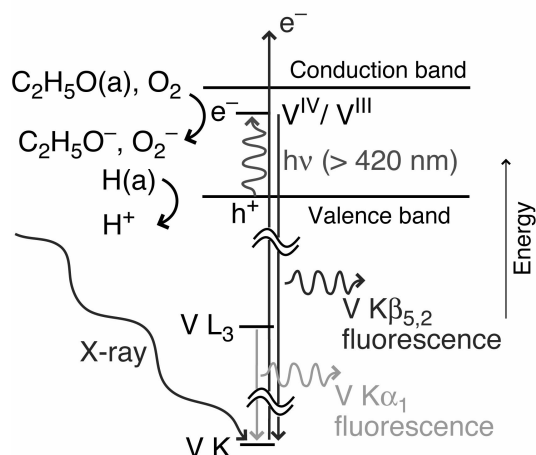


**FIGURE 1. Energy diagram of V Kβ<sub>5,2</sub> and V Kα<sub>1</sub> emission processes and of catalysis over mesoporous V-TiO<sub>2</sub> under the illumination of visible light.**

ethanol. The powder was evacuated at 523 K for 2h. Specific surface area (SA) for template-washed sample was as much as  $1200 \text{ m}^2\text{g}^{-1}$  and gradually decreased to  $800 \text{ m}^2\text{g}^{-1}$  as the V loading increased to 3 wt% V. The loading was fixed to 3.0 wt% V throughout this paper. Mesopores with narrow size distribution of  $\approx 3 \text{ nm}$  dominated. Following similar route, mesoporous  $\text{TiO}_2$  was synthesized from compounds **2** and **3**. Mesoporous  $\text{TiO}_2$  was impregnated with compound **1** in 2-propanol.

Ethanol oxidation was performed in a closed circulating system (internal volume 132 ml) equipped with quartz reaction cell illuminated with xenon arc lamp operated at 500 W (Ushio) and a UV-cut filter (L42, Kenko). 55  $\mu\text{mol}$  of ethanol and 110  $\mu\text{mol}$  of oxygen were reacted with 100 mg of catalyst. Catalyst test in 55  $\mu\text{mol}$  of ethanol in the absence of  $\text{O}_2$  was also performed. Separately, 72  $\mu\text{mol}$  of water was interacted with mesoporous V- $\text{TiO}_2$  catalyst for 15 min, evacuated for 15 min, and then 55  $\mu\text{mol}$  of ethanol and 110  $\mu\text{mol}$  of oxygen were introduced to the catalyst all at 290 K.

In addition to physicochemical characterization using XRD, HR-TEM, and BET, UV-visible absorption and V  $\text{K}\beta_{5,2}$ -selecting XAFS were studied with the concept as illustrated in Figure 1 (Izumi et al., 2007). The X-ray measurements were performed at KEK-PF 7C at 290 K. Si(111) monochromator was used and the X-ray beam was fully tuned and focused at sample position. The X-ray fluorescence from sample was analyzed by a homemade fluorescence spectrometer equipped with spherically-bent Johann-type Ge(422) crystal (Izumi, Nagamori et al., 2005). V  $\text{K}\beta_{5,2}$ -selecting V K-edge XAFS spectrum was measured by tuning the fluorescence spectrometer at fixed emission energies around V  $\text{K}\beta_{5,2}$  emission peak.

In the V  $\text{K}\beta_{5,2}$ -selecting XAFS, greater chemical shifts are utilized for state discrimination among  $\text{V}^{\text{III}}$ ,  $\text{V}^{\text{IV}}$ , and  $\text{V}^{\text{V}}$  compared to V  $\text{K}\alpha_1$  emission (Izumi, Kiyotaki et al., 2005).

## RESULTS AND DISCUSSION

**Ethanol Oxidation.** Under visible light in ethanol and  $\text{O}_2$ , selective dehydration reaction of ethanol proceeded over mesoporous V+ $\text{TiO}_2$  catalysts ( $23 - 212 \mu\text{mol h}^{-1}\text{g}_{\text{cat}}^{-1}$ ) to form water and acetaldehyde (Figure 2B, C) compared to inactive mesoporous  $\text{TiO}_2$  ( $2.3 - 16 \mu\text{mol h}^{-1}\text{g}_{\text{cat}}^{-1}$ , Figure 2A) or dehydrogenation over major anatase  $\text{TiO}_2$ -based catalysts ( $4.9 - 19 \mu\text{mol}_{\text{acetaldehyde}}\text{h}^{-1}\text{g}_{\text{cat}}^{-1}$ ; no/negligible water formation) (Masih et al., 2007). Especially, water formation in the first 1h was explosively faster ( $141 - 212 \mu\text{mol h}^{-1}\text{g}_{\text{cat}}^{-1}$ ) (Figure 2B, C) by more than one order of magnitude than

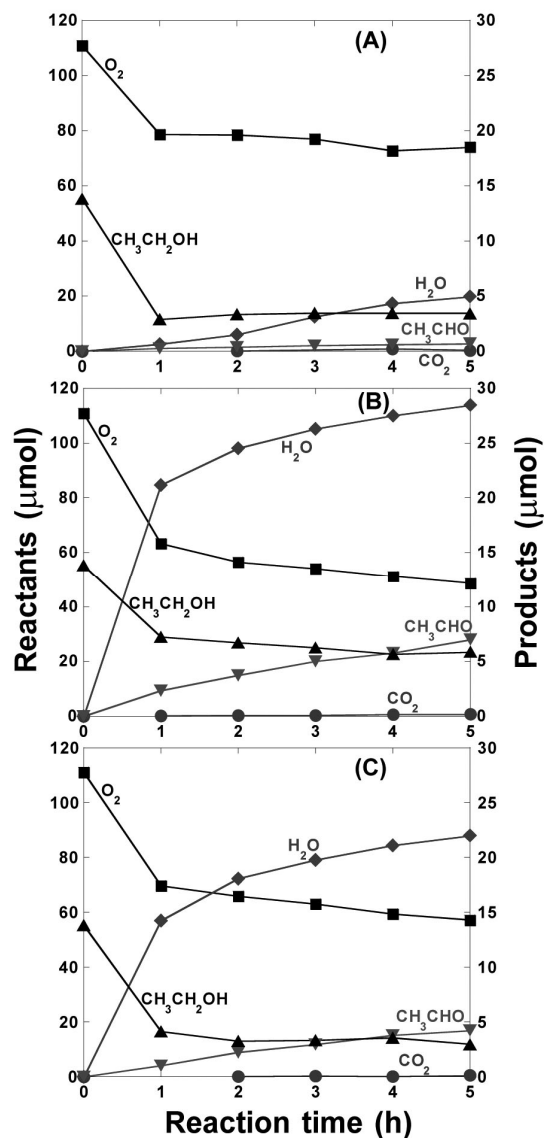


**FIGURE 2.** Ethanol oxidation reaction as a function of time under the illumination of visible light on mesoporous  $\text{TiO}_2$  (A), mesoporous V- $\text{TiO}_2$  (B), and V/mesoporous- $\text{TiO}_2$  catalysts (C) at 290 K. Ethanol (1.33 kPa) and  $\text{O}_2$  (2.67 kPa) were introduced in the closed circulation system.

steady acetaldehyde/water formation after 1h over mesoporous V-TiO<sub>2</sub> and V/mesoporous-TiO<sub>2</sub>. The steady reaction formula was



Comparative reaction only in ethanol was performed on mesoporous V-TiO<sub>2</sub> catalyst under the illumination of visible light (Figure 3A). The formation rate of acetaldehyde was 1.7 μmol h<sup>-1</sup>g<sub>cat</sub><sup>-1</sup>, only 7% of steady formation rate in ethanol + O<sub>2</sub>. No water formation was found. Hence, dehydration reaction mechanism in ethanol + O<sub>2</sub> was totally different from dehydrogenation reaction in the absence of O<sub>2</sub> over the catalyst.

Ethanol oxidation reaction was done after water adsorption on the catalyst (Figure 3B). The formation rate of acetaldehyde was 7.0 μmol h<sup>-1</sup>g<sub>cat</sub><sup>-1</sup>, 30% of steady formation rate for fresh catalyst. Again, no water was produced. Thus, remarkably active V sites for explosive dehydration reaction may be blocked by water molecules. The explosive, quick reaction in the first 1h may stabilize to constant state (Figure 2B, C) due to the blocking effect of water molecules produced.

**UV-visible Absorption Spectra.** The wavelength of light absorption gradually shifted to visible light region (beyond 400 nm) on going from major anatase TiO<sub>2</sub> or mesoporous TiO<sub>2</sub> to mesoporous V-TiO<sub>2</sub> and as the impregnated V amount increased (Masih et al., 2007).

**V Kβ<sub>5,2</sub> Emission Spectra.** The V Kβ<sub>5,2</sub> emission spectra were measured for mesoporous V-TiO<sub>2</sub> with the excitation energy set at 5484.1 eV. Intense peak top for fresh sample at 5462.1 eV shifted progressively toward lower-energy side to 5461.6 eV in ethanol, then to 5461.0 eV in ethanol under visible light. After the visible light was turned off, the peak top position increased to 5461.6 eV. Then, sample was exposed to oxygen and illuminated by visible light. The peak top further increased to 5462.4 eV. These peak top energies corresponded to V<sup>IV</sup> states (5460.5 – 5462.3 eV; Izumi et al., 2007). A shoulder peak on lower energy side at 5456 – 5460 eV constantly appeared in these emission spectra.

**V Kβ<sub>5,2</sub>-selecting XAFS Spectra Tuned to V Kβ<sub>5,2</sub> Peak Top.** Next, V Kβ<sub>5,2</sub>-selecting XANES (X-ray absorption near-edge structure) spectra were measured for mesoporous V-TiO<sub>2</sub> catalyst (Figure 4). The tune energy of fluorescence spectrometer was first fixed to each peak top to observe site structure changes systematically under each catalytic condition.

For the fresh sample, the pre-edge peak

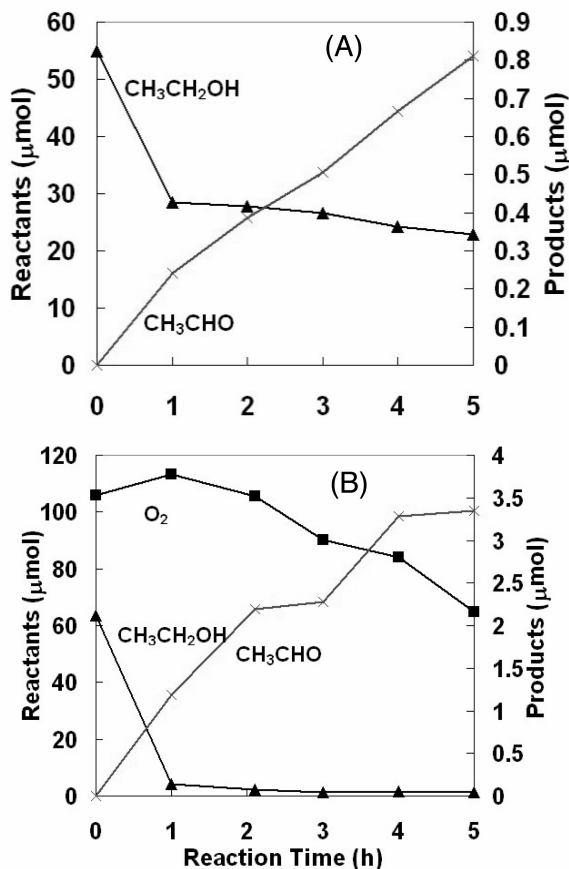


**FIGURE 3.** Ethanol oxidation reaction as a function of time under the illumination of visible light on mesoporous V-TiO<sub>2</sub> catalyst at 290 K. (A) Only ethanol (1.33 kPa) was introduced. (B) Ethanol (1.33 kPa) and O<sub>2</sub> (2.67 kPa) were introduced after water (1.73 kPa) adsorption.

and rising edge energy values were 5468.2 and 5479.7 eV, respectively (Figure 4a). These were within the ranges of corresponding values, 5467.7 – 5469.4 and 5476.9 – 5479.8 eV, respectively, for  $V^{IV}$  standard compounds, mesoporous  $V-TiO_2$  ( $V K\alpha_1$ -selecting XANES) (Izumi, Kiyotaki, et al., 2005), and mesoporous  $TiO_2$  ( $Ti K$ -edge XANES shifted by +499.8 eV) (Yoshitake et al., 2002). In combination with the  $V K\beta_{5,2}$  emission data, it was demonstrated that  $V^{IV}$  sites substituted on the  $Ti$  sites of amorphous  $TiO_2$  matrix for incipient catalyst (Figure 5a). This structure was supported by the curve fit analyses for  $V K$ -edge EXAFS (extended XAFS) [ $N(V-O) = 4 - 5$ ] (Izumi, Kiyotaki, et al., 2005; Yoshitake et al., 2003).

With the introduction of ethanol, rising edge shifted toward lower energy to 5478.0 eV (Figure 4b). A part of vanadium sites were reduced from native IV state due to the dissociative adsorption of ethanol on  $V^{IV}$  sites (Figure 4b). Pre-edge and post-edge peak positions and pattern were similar to those for fresh sample (Figure 4a).

Next, when visible light was illuminated, the rising edge further shifted toward lower energy side to 5477.8 eV (Figure 4c). Because the rising edge positions were observed at 5469.9 – 5474.7, 5476.9 – 5479.8, and 5478.0 – 5482.1 eV for  $V^{III}$ ,  $V^{IV}$ , and  $V^V$  standard inorganic compounds, respectively (Izumi, Kiyotaki et al., 2005; Wong et al, 1984), majority of  $V$  sites were  $V^{IV}$  state in this catalytic condition.

When the visible light was turned off, the edge position increased to 5479.0 eV and the pre-edge peak intensity at 5468.0 eV became fairly weak (0.21) (Figure 4d). With the introduction of oxygen under visible light, the X-ray absorption edge further shifted up to 5479.9 eV (Figure 4e – f). Partially reduced  $V$  sites due to the dissociative adsorption of ethanol and/or visible light illumination completely oxidized back to  $V^{IV}$  state in oxygen and/or visible light. Re-oxidized  $V^{IV}$  sites after the visible light was turned off were of relatively higher symmetry based on mainly  $1s \rightarrow 3d$  pre-edge peak intensity (Figure 4f, a).

In summary,  $V K\beta_{5,2}$ -selecting XANES spectra under each catalytic condition in Figure 4a, b, c, and f were assigned to catalytic reaction states of Figure 5a, b, b + c, and a, respectively.

**$V K\beta_{5,2}$ -selecting XAFS Spectra Tuned to Lower-energy Shoulder of  $V K\beta_{5,2}$ .** For partially reduced mesoporous  $V-TiO_2$  sample for Figures 4d, the fluorescence spectrometer was tuned to 5456.3 eV (lower-energy side shoulder) to specifically discriminate  $V^{III}$  state and compare to XANES spectrum tuned to  $V K\beta_{5,2}$  peak top. The obtained  $V K$ -edge XANES spectrum was depicted in Figure 6b in comparison with spectrum a tuned to 5461.6 eV (a). The spectral pattern above 5473 eV was most

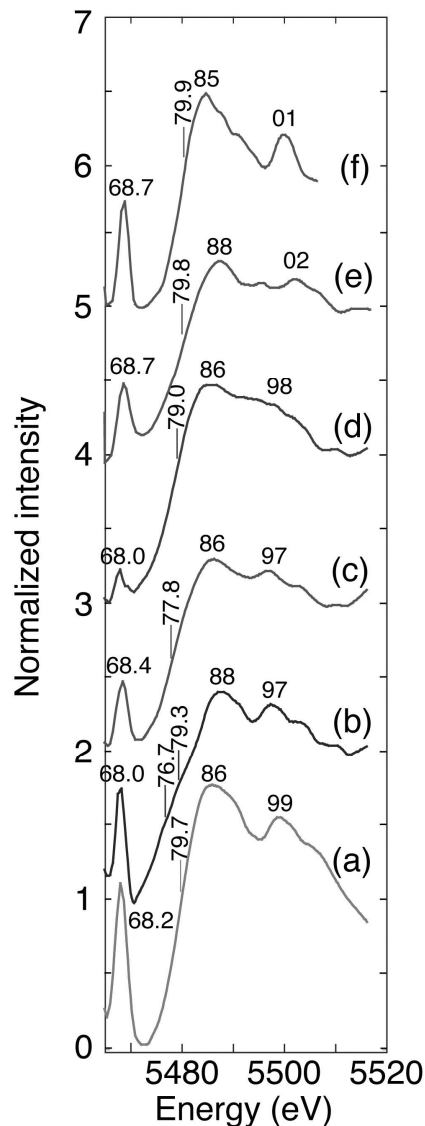


**FIGURE 4.  $V K\beta_{5,2}$ -detecting  $V K$ -edge XANES spectra for mesoporous  $V-TiO_2$  catalyst. (a) Fresh sample in argon, (b) in 2.1 kPa of ethanol, (c) in ethanol under visible light illumination, (d) after the visible light was turned off, (e) in 101 kPa of  $O_2$ , and (f) in  $O_2$  under visible light illumination. The tune energy was 5462.1, 5461.6, 5461.0, 5461.6, 5462.4, and 5462.4 eV, respectively.**

similar to the weighted sum of standard spectra for  $V^{III}$  and  $V^{IV}$  with the mixing ratio 6:4 ( $R_f = 1.1\%$ ; Figure 6, inset). The V sites for the two model compounds are surrounded with 5 – 6 O atoms similar to the V site coordination for mesoporous  $V-TiO_2$ . Thus, fully reduced  $V^{III}$  state by excited electrons under visible light was not directly detected with this trial.

The V  $K\beta_{5,2}$ -selecting XAFS measurements to directly detect  $V^{III}$  state with continuous feed of saturated pressure of ethanol gas under the illumination of visible light are in progress. When each spectral data for  $V^{III}$  and  $V^{IV}$  states will be available for mesoporous  $V-TiO_2$  catalyst, the population of each state can be determined under each catalytic condition.

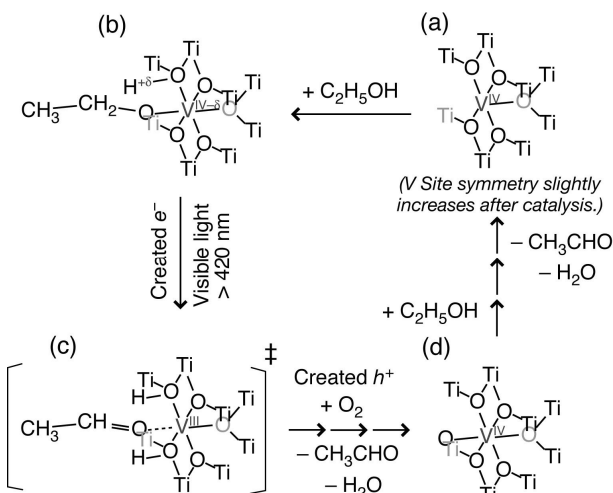


**FIGURE 5. Proposed reaction mechanism of ethanol dehydration over mesoporous  $V-TiO_2$  catalyst under visible light (a – d).**

## CONCLUSIONS

In ethanol oxidation reaction under the illumination of visible light, ethanol dehydration and dehydrogenation proceeded on mesoporous  $V+TiO_2$  and  $V+TiO_2$  (mainly anatase) catalysts, respectively. Distorted  $V^{IV}$  sites were found to be highly active to drastically evolve water in first 1h of reaction. The differences of specific SA and NHE for red-ox pair  $V^{IV} \leftrightarrow V^{III}$  (+0.337 V) compared to  $V^V \leftrightarrow V^{IV}$  for most of supported V catalysts (+0.958 V) may be also critical. Ethanol dehydration reaction chosen as a simplified model reaction on mesoporous  $V-TiO_2$  catalyst will be extended to organic solvent/dye decomposition at C–O or C–N bond(s) to reduce environmental risk.

Partial reduction of native  $V^{IV}$  sites in mesoporous  $V-TiO_2$  was observed in V  $K\beta_{5,2}$  emission and  $K\beta_{5,2}$ -selecting XANES spectra in ethanol under visible light illumination. The V state oxidized back to initial  $V^{IV}$  state in oxygen and/or under visible light. The V site symmetry (coordination) slightly increased after the photo-catalysis based on the decrease of V K pre-edge peak intensity.

The extraction of photo-reduced  $V^{III}$  states was 60% by tuning fluorescence spectrometer to 5456.3 eV for partially reduced mesoporous  $V-TiO_2$  with smaller population of  $V^{III}$  state in dynamic equilibrium with major  $V^{IV}$  + photo-excited  $e^-$  ( $\approx 10^2$  ps; Martin et al., 1994).

V doping was effective to create  $V^{IV/III}$  impurity energy level for visible light absorption between relatively greater band gap of mesoporous  $TiO_2$  due to quantum size effect. Catalytic superiority of

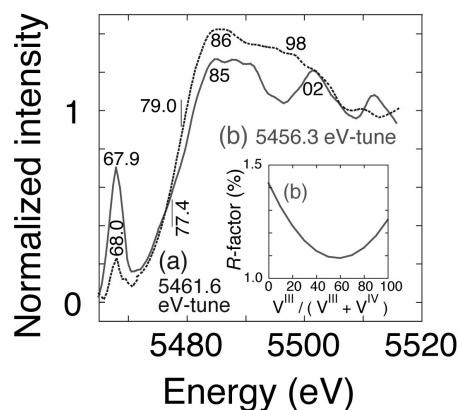


**FIGURE 6.  $V K\beta_{5,2}$ -detecting V K-edge XANES spectra for mesoporous  $V-TiO_2$  catalyst after visible light illumination in 2.1 kPa of ethanol. The fluorescence tune energy was 5461.6 (a) and 5456.3 eV (b). (Inset)  $R$ -factor change of fit to spectrum b with those for  $V^{III}_2O_3$  and  $V^{IV}O(SO_4)_nH_2O$ . The fits were performed in energy range above 5473 eV.**

ultimately exposed (catalytically available) native V<sup>IV</sup> sites was also suggested.

## ACKNOWLEDGEMENTS

X-ray measurements were performed under the approval of the Photon Factory Proposal Committee (2005P014, 2006G097). This work was financially supported from the Grant-in-aid on the Priority Area "Molecular Nano-dynamics" (Y.I. 432-17034013).

## REFERENCES

- Aita, Y.; Komatsu, M.; Yin, S.; and Sato, T. 2004. "Phase-compositional control and visible light photocatalytic activity of nitrogen-doped titania via solvothermal process". *J. Solid State Chem.* 177: 3235 – 3238.
- Anpo, M. 2004. "Preparation, Characterization, and Reactivities of Highly Functional Titanium Oxide-Based Photocatalysts Able to Operate under UV–Visible Light Irradiation: Approaches in Realizing High Efficiency in the Use of Visible Light". *Bull. Chem. Soc. Jpn.* 77(8): 1427 – 1442.
- Hou, X. G.; Hao, F. H.; Fan, B.; Gu, X. N.; Wu, X. Y.; Liu, A. D. 2006. "Modification of TiO<sub>2</sub> photocatalytic films by V<sup>+</sup> ion implantation". *Nucl. Instru. Meth. Phys. Resear. B.* 243: 99 – 102.
- Iketani, K., Sun, R. D., Toki, M., Hirota, K., and Yamaguchi, O. 2004. "Sol-gel-derived V<sub>x</sub>Ti<sub>1-x</sub>O<sub>2</sub> films and their photocatalytic activities under visible light irradiation". *Mater. Sci. Eng. B.* 108: 187 – 193.
- Izumi, Y., Konishi, K., Miyajima, T., and Yoshitake, H. 2007. "Photo-oxidation over mesoporous V-TiO<sub>2</sub> catalyst under visible light monitored by vanadium Kβ<sub>5,2</sub>-selecting XANES spectroscopy". *Mater. Lett.*, in press.
- Izumi, Y.; Kiyotaki, F.; Yagi, N.; Vlaicu, A. M., Nisawa, A.; Fukushima, S.; Yoshitake, H.; Iwasawa, Y. 2005. "X-ray Absorption Fine Structure Combined with X-ray Fluorescence Spectrometry. Part 15. Monitoring of Vanadium Site Transformations on Titania and in Mesoporous Titania by Selective Detection of the Vanadium Kα<sub>1</sub> Fluorescence", *J. Phys. Chem. B.* 109: 14884 – 14891.
- Izumi, Y.; Nagamori, H.; Kiyotaki, F.; Masih, D.; Minato, T.; Roisin, E.; Candy, J. P.; Tanida, H.; Uruga, T. 2005. "X-ray Absorption Fine Structure Combined with X-ray Fluorescence Spectrometry. Improvement of Spectral Resolution at the Absorption Edges of 9 – 29 keV". *Anal. Chem.* 77(21): 6969 – 6975.
- Khan, S. U. M., Al-Shahry, M., and Ingler, Jr., W. B. 2002. "Efficient Photochemical Water Splitting by a Chemically Modified n-TiO<sub>2</sub>". *Science.* 297: 2243 – 2245.
- Klosek, S., and Raftery, D. 2001. "Visible Light Driven V-Doped TiO<sub>2</sub> Photocatalyst and Its Photooxidation of Ethanol". *J. Phys. Chem. B.* 105(14): 2815 – 2819.
- Martin, S. T., Morrison, C. L., and Hoffmann, M. R. 1994. "Photochemical Mechanism of Size-Quantized Vanadium-Doped TiO<sub>2</sub> Particles". *J. Phys. Chem.* 98(51): 13695 – 13704.
- Masih, D., Yoshitake, H., and Izumi, Y. 2007. "Photo-oxidation of ethanol on mesoporous vanadium-titanium oxide catalysts and the relation to vanadium(IV) and (V) sites". *Appl. Catal. A.* 325(2): 276 – 282.
- Wong, J., Lytle, F. W., Messmer, R. P., and Maylotte, D. H. 1984. "K-edge absorption spectra of selected vanadium compounds". *Phys. Rev. B.* 30(10): 5596 – 5610.
- Wu, J. C. S., and Chen, C. H. 2004. "A visible-light response vanadium-doped titania nanocatalyst by sol-gel method". *J. Photochem. Photobio. A.* 163: 509 – 515.

Yamashita, H.; Ichihashi, Y.; Takeuchi, M.; Kishiguchi, S.; Anpo, M. 1999. "Characterization of metal ion-implanted titanium oxide photocatalysis operating under visible light irradiation". *J. Synchrotron Radiat.* 6: 451 – 452.

Yoshitake, H., and Tatsumi, T. 2003. "Vanadium Oxide Incorporated into Mesoporous Titania with a BET Surface Area above 1000 m<sup>2</sup>•g<sup>-1</sup>: Preparation, Spectroscopic Characterization, and Catalytic Oxidation". *Chem. Mater.* 15(8): 1695 – 1702.

Yoshitake, H., Sugihara, T., Tatsumi, T. 2002. "Preparation of Wormhole-like Mesoporous TiO<sub>2</sub> with an Extremely Large Surface Area and Stabilization of Its Surface by Chemical Vapor Deposition". *Chem. Mater.* 14(3): 1023 – 1029.

### SIGNIFICANCE OF PASSIVE SAMPLERS (POCIS) FOR WATER MONITORING OF THE RIVER TALL

*Jaswinder Kaur* (The Queens University of Belfast, Northern Ireland, United Kingdom)

Anthony Gravell (Environment Agency, Llanelli, United Kingdom)

Samuel H Mitchell (Agri-Food and Bioscience Institute, Belfast, Northern Ireland, United Kingdom)

Conventional water sampling techniques (grab sampling, spot sampling etc.) have serious limitations that can be overcome by more advanced passive sampling devices. The major drawbacks of these screening techniques include poor representation of actual concentration due to short sampling period (few minutes), availability of small samples (1-2L) for residue extraction and loss of pesticide residues during multi-step procedure of sample collection, storage, extraction and analysis. Alternatively, polar organic chemical integrative sampler (POCIS) can provide a clear representation of the presence of polar pesticides owing to their ability to monitor a water body for extended periods (days to weeks) continuously adsorbing residues. POCIS can also provide episodic data over a longer period of time with less resource than conventional techniques.

During this project, we deployed POCIS (*admixture*) for 2-4 weeks at three different sites of the River Tall (Co. Armagh, Northern Ireland) at 6 different intervals. The disks were extracted using 1:1:8 methanol:toluene:dichloromethane solvent and residues were quantified by LC-MS/MS. The time weighted average concentration (TWAC) for these contaminants were quantified on the basis of flow rate data modelled for the River Tall from an analogous reference gauged catchment (River Callan, Co. Armagh) using Flow Estimation Model. A few assumptions were made during flow rate estimation: 1) geology, soil profile, land use, altitude and slope were homogenous across the gauged (Callan) and ungauged (Tall) catchments, 2) rainfall distribution and intensity over the sampling periods were homogenous, and 3) relationship between the observed flows on the gauged and ungauged catchments are representative of the full range of flows exhibited. The data generated since May 2006 to Dec 2006 showed presence of atrazine, simazine, ethylene thiourea, terbutryn, carbendzim, diuron, isoproturon and monuron at parts per trillion levels in the River Tall.